50th AIAA Aerospace Sciences Meeting including the New Horizons Forum and Aerospace Exposition
09 - 12 January 2012, Nashville, Tennessee
AIAA 2012-1172

Flow and sound fields of initially tripped jets at Reynolds numbers ranging from 25,000 to 200,000

Christophe Bogey[*], **Olivier Marsden**[†] and **Christophe Bailly**[‡]
Laboratoire de Mécanique des Fluides et d'Acoustique
UMR CNRS 5509, Ecole Centrale de Lyon
69134 Ecully, France

The effects of the Reynolds number on initially highly disturbed isothermal round jets at Mach number M = 0.9 and at diameter-based Reynolds numbers $\mathrm{Re}_D = 2.5 \times 10^4$, 5×10^4, 10^5 and 2×10^5 are investigated using Large-Eddy Simulation. The jets originate from a pipe nozzle of radius r_0, in which a tripping procedure is applied to the boundary layers. At the nozzle exit, laminar-like mean velocity profiles of momentum thickness $\delta_\theta \simeq 0.018 r_0$, yielding Reynolds numbers Re_θ varying from 251 to 1830 depending on Re_D, and peak turbulence intensities around 9% of the jet velocity, are thus obtained. With increasing Reynolds number, the turbulence spectra close to the nozzle exit and in the mixing layers broaden, as expected, while remaining dominated by the large-scale components naturally observed in turbulent boundary layers and shear layers, respectively. The mixing layers however develop more slowly, with reduced levels of velocity fluctuations. The axial profiles of turbulence intensities become smoother, showing in particular a clear overshoot two radii downstream of the nozzle exit at $\mathrm{Re}_D = 2.5 \times 10^4$, but a monotonical growth at $\mathrm{Re}_D = 2 \times 10^5$. The jet potential core moreover lengthens slightly with Re_D, but the flow properties do not change significantly farther downstream. The jets at higher Reynolds numbers are finally found to generate lower sound levels, with a decrease of about 2 dB over the range of Re_D considered.

I. Introduction

For at least fifty years, and since pioneering works such as those by Sato[1] and Mollö-Christensen & Narasimha,[2] the Reynolds number has been recognized as an important parameter in jets as far as both flow development and sound emission are concerned. In round jets in particular, if turbulent features are classically expected to be independent of the Reynolds number provided it is sufficiently high, the effects of the diameter-based Reynolds number $\mathrm{Re}_D = u_j D/\nu$, where u_j, D and ν are the jet velocity, nozzle diameter and kinematic molecular viscosity, respectively, have been found to be strong for $\mathrm{Re}_D \lessapprox 10^5$ as pointed out in the review papers by Crighton[3] and Hussain.[4]

The influence of the Reynolds number on jet flows has been clearly described in a number of studies for jets at low Reynolds numbers, typically lower than 5×10^4, which are naturally in a fully laminar initial state. Theoretical analyses conducted by Morris[5,6] and Michalke[7] based on the linear stability equations have for instance shown that increasing the Reynolds number raises the growth rates of instability waves. A large amount of experimental data have also been obtained for plane and round jets by Lemieux,[8] Namer & Ötügen,[9] Weisgraber & Liepmann,[10] Papadopoulos & Pitts,[11] Kwon & Seo,[12] Deo *et al.*[13] and Fellouah *et al.*[14] Higher Reynolds numbers generally result in a broadening of the turbulence spectra, shorter jet potential cores, lower rates of centerline velocity decay and jet spreading, and reduced peak rms levels of velocity fluctuations.

For jets at moderate Reynolds numbers, roughly between 5×10^4 and 5×10^5, the effects of the Reynolds number may still be significant, but they are more difficult to investigate. Such jets are indeed usually in a

[*]CNRS Research Scientist, AIAA Member, christophe.bogey@ec-lyon.fr
[†]Assistant Professor at Ecole Centrale de Lyon, AIAA Member, olivier.marsden@ec-lyon.fr
[‡]Professor at Ecole Centrale de Lyon & Institut Universitaire de France, Senior AIAA Member, christophe.bailly@ec-lyon.fr

transitional initial state, characterized by appreciable levels of velocity disturbances at the nozzle exit, which tend to vary with the Reynolds number as reported in a series of experiments by Zaman.[15–17] Changing the Reynolds number in this case alters the initial turbulence conditions, which might lead to modifications of the jet characteristics exceeding those due to the Reynolds number alone. This issue, which was mentioned by Hussain & Zedan[18,19] and Gutmark & Ho,[20] among others, may be one of the reasons why there have been intense controversies about the persistence and excitability of coherent turbulent structures in laboratory-scale mixing layers and jets at moderate Reynolds numbers. On this matter, the reader may refer to the results and discussions available in the papers by Crow & Champagne,[21] Brown & Roshko,[22] Chandrsuda *et al.*,[23] Wygnanski *et al.*,[24] Zaman & Hussain,[25,26] Crighton,[3] Hussain[4] and Zaman.[16]

Concerning the sensitivity of jet noise to Reynolds number, it can first be noted that similarities have been observed experimentally between acoustic field measurements for jets at low, moderate and high Reynolds numbers. This is particularly true for supersonic jets, in which instability waves and large turbulent scales play prominent roles in noise generation as explained by Tam,[27] and spectacularly illustrated by the experimental data of Morrison & McLaughlin[28] and Troutt & McLaughlin[29] for jets at Mach numbers around 2 and Reynolds numbers $\mathrm{Re}_D = 7.9 \times 10^3$, 7×10^4 and 2.6×10^6. For these jets, indeed, the sound spectra at high Re_D have quite broadband shapes whereas the spectra at low Re_D are dominated by a narrow band of frequencies, but they exhibit coincident peak Strouhal numbers.

For subsonic jets, some similarities remain between the sound fields of low and high Reynolds number jets as evidenced by the data obtained by Stromberg *et al.*[30] for a Mach number 0.9 jet at $\mathrm{Re}_D = 3.6 \times 10^3$. It is however well known that the spectral properties of subsonic jet noise vary appreciably with the Reynolds number below a threshold value between $\mathrm{Re}_D = 10^5$ and $\mathrm{Re}_D = 4 \times 10^5$ according to different authors such as Yamamoto & Arndt,[32] Long & Arndt,[33] Bridges & Hussain[34] and Viswanathan.[35] Unfortunately, the effects of the Reynolds number alone are relatively complicated to identify because, as indicated previously, they may be overwhelmed by the effects of other parameters dependent on Re_D. These parameters include the nozzle-exit boundary-layer thickness and disturbance levels, which have been found to have a major impact on subsonic jet noise in the experiments of Mollo-Christensen *et al.*[31] and Zaman,[15,16] as well as in the simulations of Bogey & Bailly[36] and Bogey *et al.*[37] for instance, especially regarding the contribution of shear-layer vortex pairings.

In light of the above, therefore, there appears to be a need to quantify the influence of the Reynolds number on subsonic jets at moderate Reynolds numbers, and that the only proper way to do it is to consider jets with effectively the same initial parameters except for the Reynolds number. To achieve this, the use of simulations as numerical experiments under highly controlled conditions seems natural based on progress in the computations of compressible jets, see in Colonius & Lele,[38] Bailly & Bogey[39] and Wang *et al.*[40] for example. Direct Numerical Simulations (DNSs) or Large-Eddy Simulations (LESs) can be performed, as was the case in past studies by Freund,[41] Bogey *et al.*,[42] Klein *et al.*,[43] Bogey & Bailly,[44,45] Kleinman & Freund,[46] and Kim & Choi.[47] The last five references[43–47] are particularly relevant here because they demonstrated the feasibility of investigating Reynolds number effects in mixing layers or jets at low or moderate Reynolds numbers by means of simulations. The flow initial state was nevertheless laminar, or weakly disturbed in these works.

In the present work, the aim is to carefully examine the influence of the Reynolds number on the flow and sound fields of subsonic jets at moderate Reynolds numbers, which are, on the contrary, initially highly disturbed. Four isothermal round jets are computed using LESs on a grid containing 252 million points using low-dissipation numerical schemes and relaxation filtering as a subgrid dissipation model. They are at a Mach number $\mathrm{M} = 0.9$, and at Reynolds numbers $\mathrm{Re}_D = 2.5 \times 10^4$, 5×10^4, 10^5 and 2×10^5, respectively. As in our recent simulations[37,48,49] of jets at a constant $\mathrm{Re}_D = 10^5$ providing practically grid-converged solutions using the same grid, the jets originate from a pipe nozzle, in which a trip-like excitation is applied to the boundary layers in order to obtain peak axial turbulence intensities $u'_e/u_j \simeq 9\%$ at the exit section. A great care is also taken to maintain, at the exit, similar laminar-like mean velocity profiles of momentum thickness $\delta_\theta \simeq 0.018 r_0$, where $r_0 = D/2$ is the pipe radius, in all cases. The present jets consequently display nearly identical initial conditions except for Re_D, and the trends revealed by the simulation data should be attributable to Reynolds number effects only.

The paper is organized as follows. In section II, the main parameters of the jets and of the simulations, including numerical algorithm, computational grids and times, are documented. In section III, the nozzle-exit flow conditions are first presented. The shear-layer and jet flow fields as well as the acoustic fields are then shown. Concluding remarks are provided in section IV.

II. Parameters

In this section, the jet inflow conditions are first defined. The numerical methods and parameters are then presented. They are identical to those used in recent jet simulations, which have been thoroughly described in previous references.[36,37,48,49] Consequently only a brief description is provided here.

The simulation of the jet at $\mathrm{Re}_D = 10^5$ considered in the present study was moreover performed for the first time and detailed in Bogey *et al.*,[48] in which a great deal of information about the boundary-layer tripping procedure, the discretization quality and the LES reliability is available. This computation is also known as Jetring1024drdz or Jet9% in other papers.[37,48,49]

A. Jet definition

Four isothermal round jets, referred to as JetRe25e3, JetRe50e3, JetRe100e3 and JetRe200e3, are investigated. They are at a Mach number $\mathrm{M} = u_j/c_a = 0.9$, where c_a is the ambient speed of sound, and at Reynolds numbers $\mathrm{Re}_D = 2.5 \times 10^4$, 5×10^4, 10^5 and 2×10^5, respectively, as reported in table 1. They originate at $z = 0$ from a pipe nozzle of radius r_0 and length $2r_0$, whose lips are $0.053r_0$ thick. The ambient temperature and pressure are $T_a = 293$ K and $p_a = 10^5$ Pa. For all jets, an axial velocity profile given by a polynomial approximation of the Blasius laminar boundary-layer profile is imposed at the pipe inlet. This profile has a thickness $\delta = 0.15r_0$, yielding a momentum thickness $\delta_\theta = 0.018r_0$ similar to those measured by Zaman[15,16] in tripped subsonic jets at $\mathrm{Re}_D \simeq 10^5$. Radial and azimuthal velocities are initially set to zero, pressure is set to p_a, and the temperature is determined by a Crocco-Busemann relation.

Table 1. Jet inflow conditions: Mach number M, Reynolds number Re_D, and inlet boundary-layer thickness δ.

	M	Re_D	δ/r_0
JetRe25e3	0.9	2.5×10^4	0.15
JetRe50e3	0.9	5×10^4	0.15
JetRe100e3	0.9	10^5	0.15
JetRe200e3	0.9	2×10^5	0.15

The jet boundary layers are tripped inside the pipe by adding random low-level vortical disturbances decorrelated in the azimuthal direction at $z = -r_0$. The excitation magnitudes are empirically chosen in order to obtain, at the pipe exit, peak turbulence intensities u'_e/u_j around 9% in all cases, as well as mean velocity profiles in fair agreement with the laminar profiles imposed at the pipe inlet, which will be illustrated in section III.A. Pressure fluctuations of maximum amplitude 200 Pa random in both space and time are also added in the shear layers between $z = 0.25r_0$ and $z = 4r_0$ from $t = 0$ up to non-dimensional time $t = 12.5r_0/u_j$ in order to speed up the initial transitory period.

B. LES procedure and numerical methods

The LESs are carried out using a solver of the three-dimensional filtered compressible Navier-Stokes equations in cylindrical coordinates (r, θ, z) based on low-dissipation and low-dispersion explicit schemes. The axis singularity is taken into account by the method of Mohseni & Colonius.[50] To alleviate the time-step restriction near the cylindrical origin, the derivatives in the azimuthal direction around the axis are calculated at coarser resolutions than permitted by the grid.[51] Fourth-order eleven-point centered finite differences are used for spatial discretization, and a second-order six-stage Runge-Kutta algorithm is implemented for time integration.[52] A sixth-order eleven-point centered filter[53] is applied explicitly to the flow variables every time step. Non-centered finite differences and filters are also used near the pipe walls and the grid boundaries.[36,54] The radiation conditions of Tam & Dong[55] are finally applied at all boundaries, with the addition at the outflow of a sponge zone combining grid stretching and Laplacian filtering.[56]

In the simulations, the explicit filtering is employed to remove grid-to-grid oscillations, but also as a subgrid high-order dissipation model to relax turbulent energy from scales at wave numbers close to the grid cut-off wave number while leaving larger scales mostly unaffected.[44,57,58] With this in mind, the reliability of the LES fields in JetRe100e3 has been studied in Bogey *et al.*[48] based on the tranfer functions associated with molecular viscosity, explicit (relaxation) filtering and time integration. Viscosity was shown to be the dominant dissipation mechanism for scales discretized at least by seven points per wavelength. The physics of

the larger structures are therefore expected not to be governed by numerical or subgrid-modeling dissipation in JetRe100e3, which implies in particular that the effective flow Reynolds number should not be artificially decreased. This remark certainly equally holds for the simulations JetRe25e3 and JetRe50e3 dealing with jets at lower Reynolds numbers using the same grid. This is also likely the case for JetRe200e3 in which the jet Reynolds number is only slightly higher than that in JetRe100e3.

C. Simulation parameters

As indicated in table 2, the LESs are performed using a grid containing $n_r \times n_\theta \times n_z = 256 \times 1024 \times 962 = 252$ million points. There are 169 points along the pipe nozzle, 77 points within the jet radius, and 31 points inside the inlet boundary layers. The physical domain, excluding the eighty-point outflow sponge zone, extends axially up to $L_z = 25r_0$, and radially up to $L_r = 9r_0$.

Table 2. Simulation parameters: numbers of grid points n_r, n_θ, n_z, mesh spacings Δr at $r = r_0$, $r_0\Delta\theta$, and Δz at $z = 0$, extents L_r, L_z of the physical domain, radial position r_c of the far-field extrapolation surface, and time duration T.

n_r, n_θ, n_z	$\Delta r/r_0$	$r_0\Delta\theta/r_0$	$\Delta z/r_0$	L_r, L_z	r_c/r_0	Tu_j/r_0
$256, 1024, 962$	0.36%	0.61%	0.72%	$9r_0, 25r_0$	6.5	375

The mesh spacing is uniform in the azimuthal direction, with $r_0\Delta\theta = 0.0061r_0$. In the axial direction, the mesh size is minimum between $z = -r_0$ and $z = 0$, with $\Delta z = 0.0072r_0$. It increases upstream of $z = -r_0$, but also downstream of the nozzle at stretching rates lower than 1% allowing to reach $\Delta z = 0.065r_0$ at $z = 13.3r_0$. In the radial direction, the mesh size is minimum around $r = r_0$, with $\Delta r = 0.0036r_0$. The maximum mesh size, obtained for $r \geq 3r_0$, is equal to $\Delta r = 0.081r_0$, yielding a Strouhal number of $\mathrm{St}_D = fD/u_j = 6.9$ for an acoustic wave discretized by four points par wavelength, where f is the time frequency.

The quality of the discretization in JetRe100e3 has been assessed in Bogey *et al.*[48] The ratios between the integral length scales of the axial fluctuating velocity and the mesh sizes along the lip line were shown to fall between 4 and 10. The properties of the nozzle-exit turbulence and of the shear-layer flow fields were moreover found to be practically grid-converged. The grid resolution is thus expected to be appropriate in JetRe100e3, as well as in JetRe25e3 and JetRe50e3 for the lower Reynolds number jets in which the contribution of fine-scale turbulence is naturally weakened. The resolution is also probably sufficient in JetRe200e3 for the jet at $\mathrm{Re}_D = 2 \times 10^5$, in which, according to classical observations in free shear flows,[4,20,22,24,26,43,46] the increase of the Reynolds number by a factor of two with respect to the jet in JetRe100e3 should produce more small-scale structures without fundamentally altering the dominant large-scale.

The simulation time, given in table 2, is equal to $375r_0/u_j$ in all cases. Density, velocity components and pressure are recorded from time $t = 100r_0/u_j$ at every point along the jet axis, and on the two surfaces at $r = r_0$ and $r = r_c = 6.5r_0$, at a sampling frequency allowing the computation of spectra up to a Strouhal number of 20. The velocity spectra are evaluated from overlapping samples of duration $27.4r_0/u_j$. The flow statistics are determined from $t = 175r_0/u_j$, and they are averaged in the azimuthal direction.

The simulations have been performed using NEC SX-8 computers, on 7 processors using OpenMP, leading to a CPU speed of around 36 Gflops. Each LES required around 7,000 CPU hours and 60 Gb of memory for 164,000 time steps.

D. Far-field extrapolation

The LES near fields are propagated to the acoustic far field by solving the isentropic linearized Euler equations (ILEE) in cylindrical coordinates.[37,48,59] The extrapolation is performed from fluctuating velocities and pressure recorded in the LESs on a surface at $r = 6.5r_0$ as mentioned above. These data are interpolated onto a cylindrical surface discretized by an axial mesh spacing of $\Delta z = 0.065r_0$. They are then imposed at the bottom boundary of the grid on which the ILEE are solved using the same numerical methods as in the LESs. This grid contains $845 \times 256 \times 1155$ points, and extends axially from $z = -16.6r_0$ to $58.2r_0$ and radially up to $r = 61.4r_0$. The grid spacings are uniform with $\Delta r = \Delta z = 0.065r_0$, yielding $\mathrm{St}_D = 8.6$ for an acoustic wave at four points per wavelength. After a propagation time of $t = 60r_0/u_j$, pressure is recorded around the jets at a distance of $60r_0$ from $z = r = 0$, where far-field acoustic conditions are expected to apply according to the experiments of Ahuja *et al.*,[60] during a period of $250r_0/u_j$. Pressure spectra are evaluated using overlapping samples of duration $38r_0/u_j$, and they are averaged in the azimuthal direction.

III. Results

A. Nozzle-exit flow conditions

The profiles of mean and rms axial velocities obtained at the nozzle exit of the jets are presented in figure 1. They appear not to vary much with the Reynolds number, and to be comparable to the profiles measured by Zaman[15,16] for a tripped jet at $\mathrm{Re}_D = 10^5$, as was intended. In figure 1(a), the mean velocity profiles are all similar to the Blasius laminar profile specified at the pipe-nozzle inlet. Small shape modifications, indicative of early stages of transition towards turbulent mean velocity profiles, are however observed as the Reynolds number decreases, leading to a shape factor ranging from $H = 2.40$ at $\mathrm{Re}_D = 2 \times 10^5$ down to $H = 2.18$ at $\mathrm{Re}_D = 2.5 \times 10^4$, refer to table 3 for all flow parameters at $z = 0$. The exit boundary-layer momentum thickness $\delta_\theta(0)$ also changes a little with Re_D. It is equal to 2.01, 1.91, 1.85, and 1.83 percent of the nozzle radius in JetRe25e3, JetRe50e3, JetRe100e3 and JetRe200e3, respectively, yielding Reynolds numbers $\mathrm{Re}_\theta = u_j \delta_\theta(0)/\nu = 251$, 477, 925 and 1830. Viscosity effects should consequently be strong in the shear layers of the jets at lower Re_D, but much weaker at higher Re_D. In figure 1(b), the rms velocity profiles show significant values over a slightly wider zone for lower Re_D, as a result of the variations of $\delta_\theta(0)$, but the peak turbulence intensity remains very close to 9% in all cases. The shear layers of the present jets are therefore characterized by nearly the same initial conditions except for the Reynolds number Re_θ. These conditions correspond to those found in highly disturbed, or nominally (not fully) turbulent, boundary layers.[15,16,18,19,49]

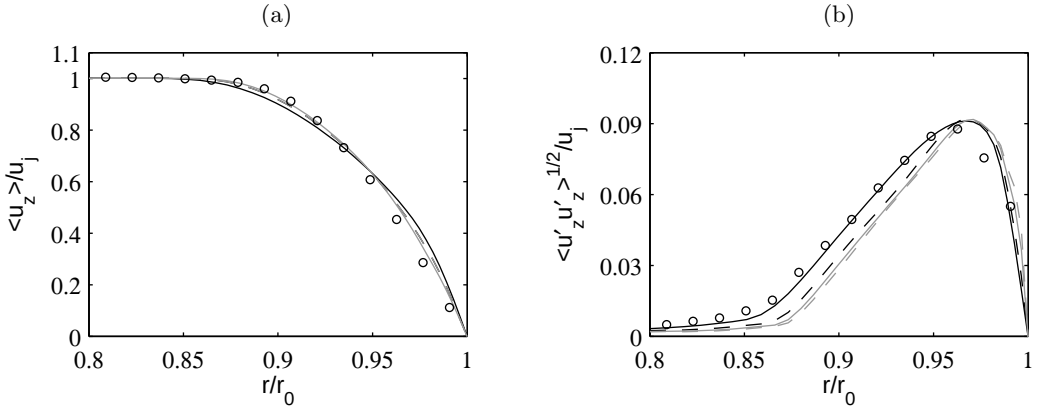

Figure 1. Profiles at $z = 0$ (a) of mean axial velocity $< u_z >$ and (b) of the rms values of fluctuating axial velocity u'_z: ——— JetRe25e3, − − − JetRe50e3, ——— JetRe100e3, – – – JetRe200e3; ∘ measurements of Zaman[15,16] for a Mach 0.18, tripped jet at $\mathrm{Re}_D = 10^5$.

As in previous references,[48,49] the properties of the jet initial disturbances are examined by calculating spectra of the fluctuating axial velocity at $r = r_0$ and $z = 0.4r_0$ just downstream of the nozzle lip. The spectra thus determined are represented as a function of the Strouhal number $\mathrm{St}_D = fD/u_j$ in figure 2(a), and of the dimensionless azimuthal wave number k_θ in figure 2(b). With increasing Reynolds number, the spectra are clearly seen to broaden, as usually happens when the effects of molecular viscosity diminish in turbulent flows. More precisely, the contributions of finer scale components, noticed here for Strouhal numbers $\mathrm{St}_D \gtrapprox 2$ and azimuthal modes $k_\theta \gtrapprox 50$, become stronger, whereas those of larger scale components are slightly reduced. The shapes of the spectra however do not change fundamentally. For all jets, indeed, the frequency spectra in figure 2(a) are rather flat up to $\mathrm{St}_D \simeq 1$ and decrease for higher Strouhal numbers. In the same way, the spectra in figure 2(b) all show a distribution of turbulent energy over a very large number of azimuthal modes with peak components centered around $k_\theta \simeq 42$, or $k_\theta \delta / r_0 \simeq 7$ when normalized by the boundary-layer thickness. As pointed out in a recent note,[49] similar spectral features were obtained for instance by Eggels *et al.*[61] for a fully turbulent pipe flow at $\mathrm{Re}_\theta = 236$, and by Tomkins & Adrian[62] for turbulent boundary layers at $\mathrm{Re}_\theta = 1015$ and 7705, that is for Reynolds numbers lying roughly within the range $\mathrm{Re}_\theta = 251 - 1830$ considered in this work. These results indicate that the large-scale structures initially dominating in the present jets are organized in a similar fashion to those naturally developing in turbulent wall-bounded flows, and that they depend negligibly on the Reynolds number.

As classically done to evaluate the size of large scales in turbulent flows, integral length scales are computed from fluctuating velocity u'_z at the same position as the previous spectra. The axial and azimuthal

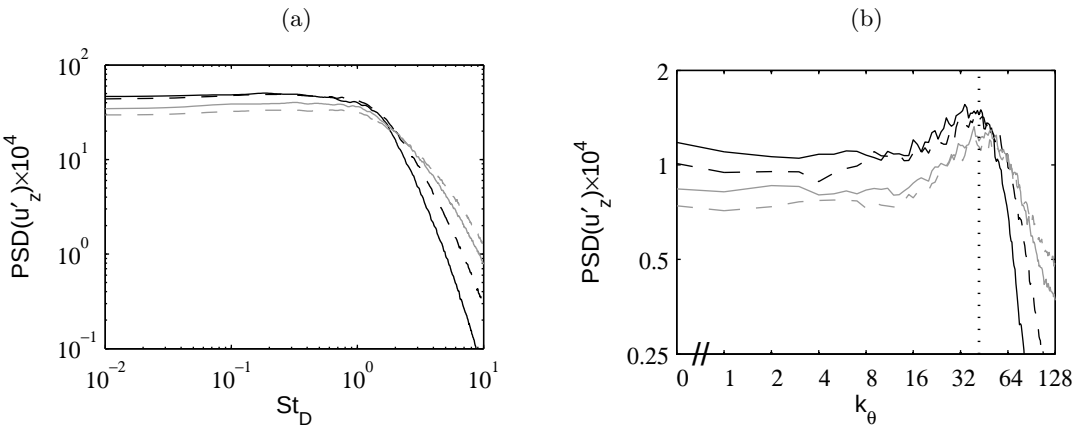

Figure 2. Power spectral densities (PSD) normalized by u_j of fluctuating velocity u'_z at $r = r_0$ and $z = 0.4r_0$, as functions (a) of Strouhal number $\mathrm{St}_D = fD/u_j$ and (b) of azimuthal wavenumber k_θ: ——— JetRe25e3, − − − JetRe50e3, ——— JetRe100e3, – – – JetRe200e3. The dotted line indicates $k_\theta = 42$.

length scales $L_{uu}^{(z)}$ and $L_{uu}^{(\theta)}$ thus obtained at $r = r_0$ and $z = 0.4r_0$ are given in table 3. They both decrease monotonically with Re_D, from $L_{uu}^{(z)} = 0.102r_0$ and $L_{uu}^{(\theta)} = 0.021r_0$ in JetRe25e3 down to $L_{uu}^{(z)} = 0.048r_0$ and $L_{uu}^{(\theta)} = 0.012r_0$ in JetRe200e3, probably due to the generation of more fine-scale structures with increasing Reynold number. The ratio $L_{uu}^{(z)}/L_{uu}^{(\theta)}$ is however noted not to vary appreciably, and to take values around 4.5 regardless of Re_D.

Table 3. Jet nozzle-exit conditions: peak turbulence intensity u'_e/u_j, shape factor H, and boundary-layer momentum thickness $\delta_\theta(0)$ at the nozzle exit, Reynolds number Re_θ based on $\delta_\theta(0)$, and integral length scales $L_{uu}^{(z)}$ and $L_{uu}^{(\theta)}$ of velocity u'_z at $r = r_0$ and $z = 0.4r_0$.

	u'_e/u_j	H	$\delta_\theta(0)/r_0$	Re_θ	$L_{uu}^{(z)}/r_0$	$L_{uu}^{(\theta)}/r_0$
JetRe25e3	9.12%	2.18	2.01%	251	0.102	0.021
JetRe50e3	9.20%	2.30	1.91%	477	0.076	0.016
JetRe100e3	9.18%	2.36	1.85%	925	0.058	0.013
JetRe200e3	9.13%	2.40	1.83%	1830	0.048	0.012

At this point, it can be interesting to compare the integral length scales with the length scales corresponding to the components dominating in the velocity spectra. At $r = r_0$ and $z = 0.4r_0$ in the jets, they are found to differ both qualitatively and quantitatively. The integral length scales indeed depend significantly on the Reynolds number, whereas the dominant length scales do not. The former are furthermore much smaller than the latter, certainly because they are based on all turbulent structures, including the finer. This is particularly true for the length scales in the azimuthal direction, in which there is about an order of magnitude discrepancy between $L_{uu}^{(\theta)} = 0.012r_0 - 0.021r_0$ and the structure spacing $\lambda_\theta \simeq 0.15r_0$ associated with the peak wavenumber $k_\theta \simeq 42$.

B. Shear-layer development

Vorticity fields obtained from the pipe-nozzle exit up to $z = 5r_0$ in the jet shear layers are represented in figure 3. For the jet at $\mathrm{Re}_D = 2.5 \times 10^4$, large-scale structures are clearly visible in figure 3(a), which is not surprising given the momentum-thickness-based Reynolds number $\mathrm{Re}_\theta = 251$ in this case. The shear layer shows structures elongated in the streamwise direction near the pipe exit, most likely corresponding to those observed in turbulent boundary layers[62,63] as discussed above and in a previous paper.[49] It seems to roll up around $z = 1.5r_0$, and then to exhibit, farther downstream, large-scale structures resembling the coherent vortical structures revealed by the well-known visualizations of Brown & Roshko.[22] With increasing Reynolds number, there is a gradual appearance of fine-scale turbulence, and large-scale structures are more difficult to distinguish, see in particular in figure 3(d) for the jet at $\mathrm{Re}_D = 2 \times 10^5$ (and $\mathrm{Re}_\theta = 1830$). The vorticity snapshots finally suggest that the shear layers develop more slowly at higher Reynolds numbers.

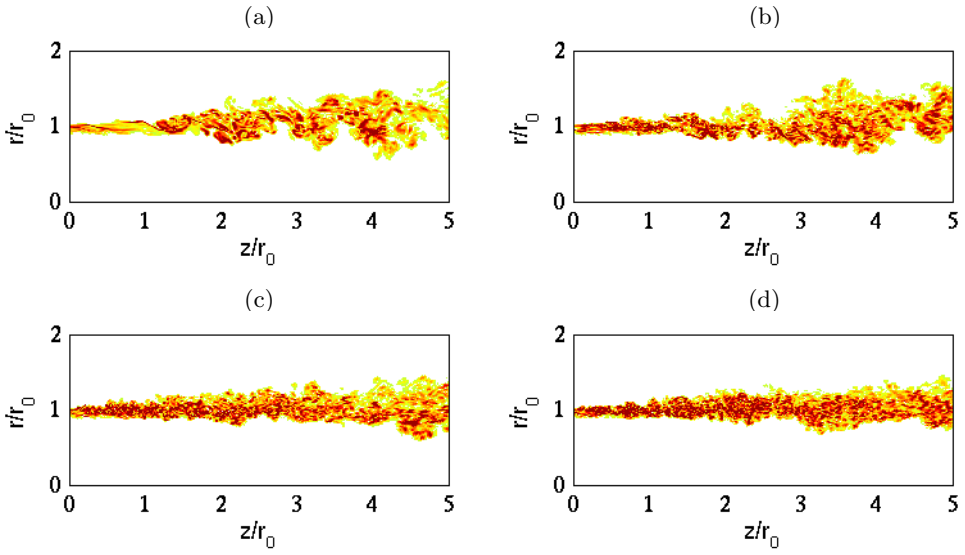

Figure 3. Snapshots in the (z, r) plane of vorticity norm $|\omega|$ in the shear layer downstream of the pipe lip up to $z = 5r_0$: (a) JetRe25e3, (b) JetRe50e3, (c) JetRe100e3, (d) JetRe200e3. The colour scale ranges up to the level of $18u_j/r_0$.

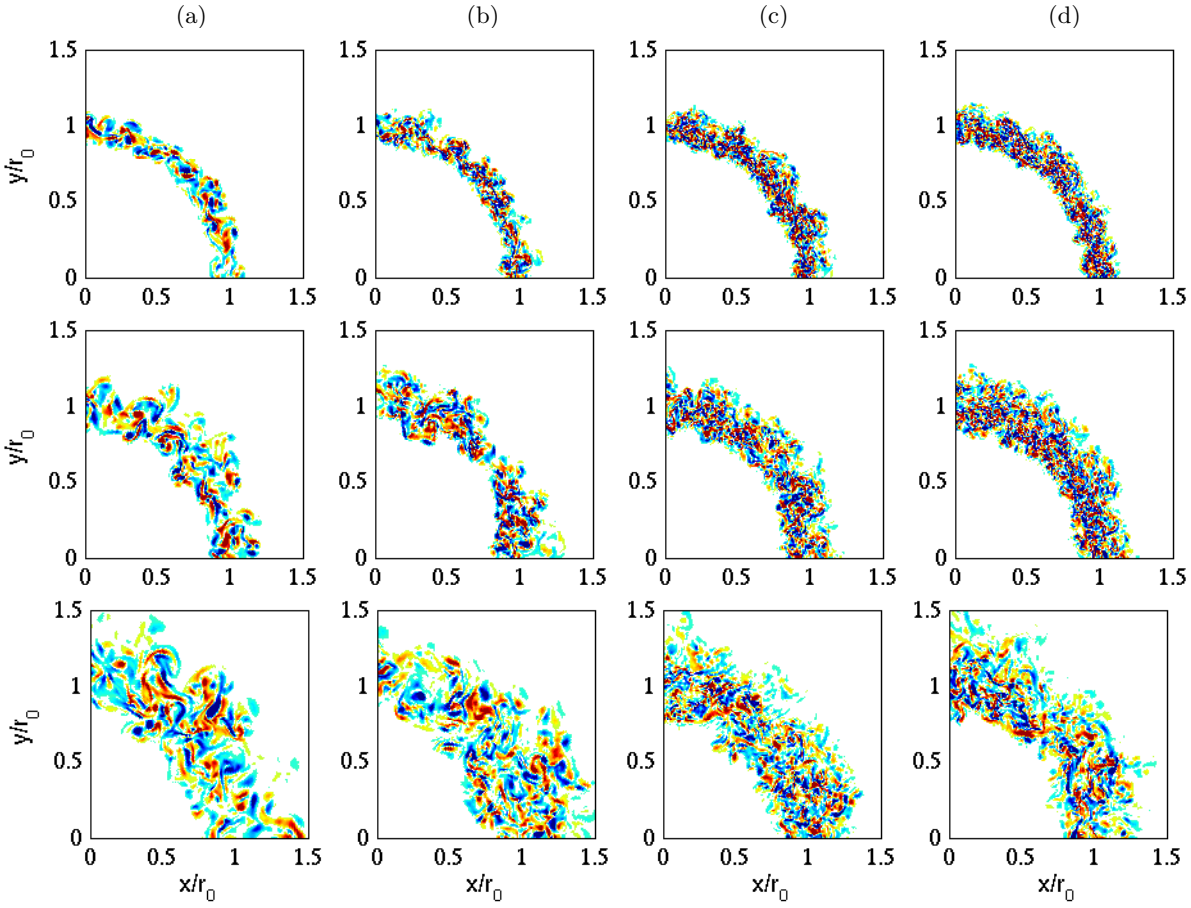

Figure 4. Snapshots in the (r, θ) or (x, y) planes at $z = r_0$, $2r_0$ and $4r_0$, from top to bottom, of axial vorticity ω_z: (a) JetRe25e3, (b) JetRe50e3, (c) JetRe100e3, (d) JetRe200e3. The colour scale ranges from levels from $-13u_j/r_0$ to $13u_j/r_0$. Only $x, y \geq 0$ is shown.

To illustrate the organization of the shear-layer turbulent structures in the azimuthal direction, snapshots of the axial vorticity ω_z obtained in three sections located at $z = r_0$, $z = 2r_0$ and $z = 4r_0$ are presented in figure 4. At the first position at $z = r_0$, the vorticity field changes appreciably as Re_D, and consequently Re_θ, vary. As was previously the case in the (x, y) plane, large-scale structures appear clearly in JetRe25e3, whereas fine-scale turbulence tends to dominate in the jets at higher Reynolds numbers. These trends persist, albeit attenuated, farther downstream at $z = 2r_0$ and $z = 4r_0$. It can also be emphasized that turbulence in the present initially highly disturbed jets is noticed to be fully three-dimensional in all three sections. There is notably no evidence of the presence of the axisymmetric or Kelvin-Helmholtz structures typically found in initially laminar jets,[36,37] even in the jet at $\mathrm{Re}_D = 2.5 \times 10^4$ displaying coherent-like vortical structures in figure 3(a).

The variations over $0 \leq z \leq 10r_0$ of the shear-layer momentum thickness δ_θ are presented in figure 5(a). In accordance with the vorticity fields of figure 3, they show that the mixing layers develop more slowly with increasing Reynolds number. To quantify this tendency, the shear-layer spreading rates $\mathrm{d}\delta_\theta/\mathrm{d}z$ are depicted in figure 5(b). Their profiles vary significantly with Re_D, in terms of both amplitude and shape. For the jet at $\mathrm{Re}_D = 2.5 \times 10^4$ (and $\mathrm{Re}_\theta = 251$), the spreading rate rapidly rises downstream of the pipe exit to reach values of around 0.03 at $z \simeq 1.5r_0$, that is the position where a rolling-up of the shear layer can be guessed in figure 3(a). It remains close to this value up to $z \simeq 4r_0$, and then decreases gently down to about 0.24 at $z = 10r_0$. At higher Reynolds numbers, the spreading rates are lower, especially during the early stage of mixing-layer growth. For the jet at $\mathrm{Re}_D = 2 \times 10^5$ (and $\mathrm{Re}_\theta = 1830$), in particular, they do not exceed 0.02 upstream of $z = 3.3r_0$. A small hump is however observed in the vicinity of the pipe exit, which is in agreement with measurements provided by Husain & Hussain[64] for initially turbulent axisymmetric mixing layers at $\mathrm{Re}_\theta \simeq 1400$. Downstream of $z \simeq 8r_0$, the spreading rates from the four jet LESs appear moreover relatively similar. This behaviour can be related to experimental results of Hussain & Zedan,[18] who obtained asymptotic spreading rates nearly independent of the Reynolds number in mixing layers at $\mathrm{Re}_\theta = 184 - 384$, all characterized initially by laminar mean velocity profiles and turbulence intensities $u'_e/u_j \simeq 6\%$.

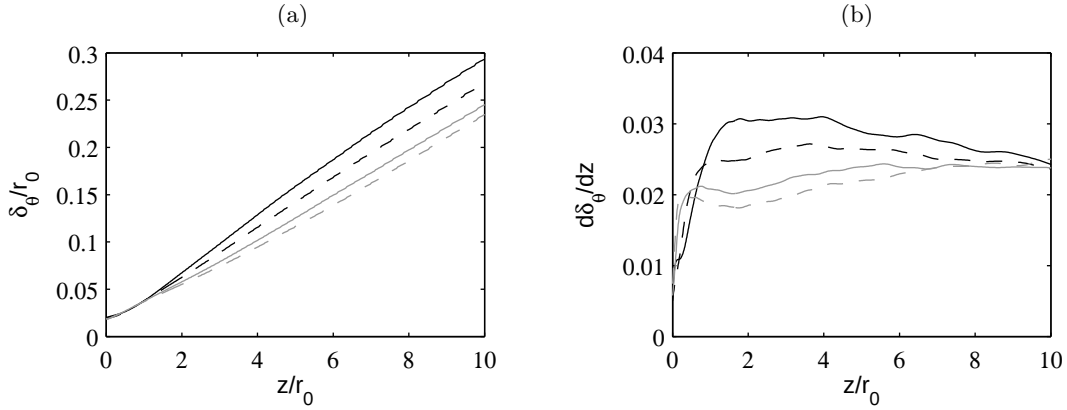

Figure 5. Axial variations (a) of shear-layer momentum thickness δ_θ and (b) of spreading rate $\mathrm{d}\delta_\theta/\mathrm{d}z$: ——— JetRe25e3, − − − JetRe50e3, ——— JetRe100e3, – – – JetRe200e3.

The peak rms values of axial, radial and azimuthal velocities u'_z, u'_r and u'_θ and the maximum Reynolds shear stresses $< u'_r u'_z >$ are represented in figure 6 between $z = 0$ and $z = 10r_0$. The profiles obtained for the jet at $\mathrm{Re}_D = 2.5 \times 10^4$ all exhibit a well-marked overshoot about two radii downstream of the nozzle exit. Peak rms values $< u'^2_z >^{1/2} = 0.173u_j$ and $< u'^2_r >^{1/2} = 0.133u_j$ are reached for example. Farther downstream, the profiles slowly decrease, and values such as $< u'^2_z >^{1/2} \simeq 0.15u_j$ and $< u'^2_r >^{1/2} \simeq 0.11u_j$ are observed at $z = 10r_0$. For higher Reynolds numbers, after a sharper initial growth, the turbulence intensity profiles become smoother. The humps located around $z = 2r_0$ are reduced, and even disappear at $\mathrm{Re}_D = 2 \times 10^5$, yielding profiles increasing monotonically in that case. As viscosity effects diminish in the shear layers, the latter consequently develop with lower turbulence intensities, leading for instance to peak rms values of u'_z and u'_r of only $0.151u_j$ and $0.111u_j$ in JetRe200e3, refer also to table 4. At larger distances from the nozzle, the fluctuation levels seem however to tend towards similar values regardless of the Reynolds number. Comparable results can be found in the paper of Hussain & Zedan.[18] For initially laminar mixing layers with constant $u'_e/u_j \simeq 6\%$ and Re_θ varying between 184 and 384, these authors indeed measured axial turbulence intensity profiles showing a hump shortly downstream of the nozzle, and then relaxing to nearly identical

values. It further appeared that the peak values are around 19% at $\mathrm{Re}_\theta = 184$ but 17% at $\mathrm{Re}_\theta = 384$, which is in line with the present LES data.

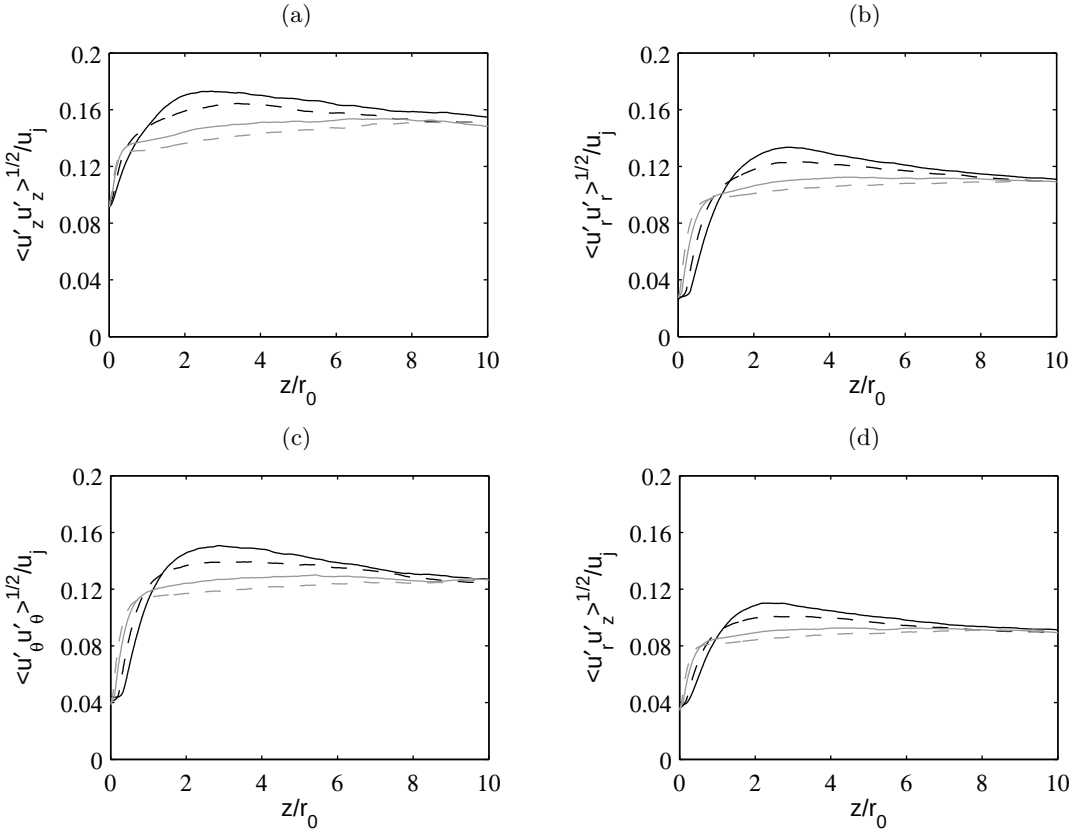

Figure 6. Variations of the peak rms values of fluctuating velocities (a) u'_z, (b) u'_r, (c) u'_θ, and (d) of the peak magnitudes of Reynolds shear stress $<u'_r u'_z>$: ——— JetRe25e3, − − − JetRe50e3, ——— JetRe100e3, – – – JetRe200e3.

Table 4. Peak values of turbulence intensities in the jets.

	$<u'^2_z>^{1/2}/u_j$	$<u'^2_r>^{1/2}/u_j$	$<u'^2_\theta>^{1/2}/u_j$	$<u'_r u'_z>/u_j$
JetRe25e3	17.3%	13.3%	15.1%	11.0%
JetRe50e3	16.4%	12.3%	13.9%	10.1%
JetRe100e3	15.4%	11.2%	13.0%	9.3%
JetRe200e3	15.1%	11.1%	12.7%	9.2%

Spectra of the radial velocity u'_r are finally computed along the lip line at the two axial positions $z = 1.5r_0$ and $z = 4r_0$, and plotted in figures 7(a) and 7(b) as a function of the Strouhal number St_D. With increasing Reynolds number, the spectra become broader, as expected. They remain however dominated by low-frequency components centered around similar Strouhal numbers, approximately equal to $\mathrm{St}_D = 1.4$ at the first position and $\mathrm{St}_D = 0.7$ at the second, yielding $\mathrm{St}_\theta = f\delta_\theta(0)/u_j = 0.012$ and $\mathrm{St}_\theta = 0.006$. The value $\mathrm{St}_\theta = 0.012$ corresponds fairly well to the frequencies which were found in theoretical analyses based on the linear stability equations,[5–7] as well as in experiments,[20] to predominate early on initially laminar annular mixing layers. For Re_θ higher than 200 and for Re_D between 10^4 and 10^5, according to Morris[5] and Gutmark & Ho,[20] respectively, these frequencies were moreover shown not to depend much on the Reynolds number, which is in the agreement with the present trends. An instability-like frequency is therefore seen to persist in the initially highly disturbed shear layers considered in this study, which can be attributed to the facts that the exit boundary layers are transitional but not fully turbulent, and that the Reynolds numbers are moderate. This component emerges very distinctly at $\mathrm{Re}_D = 2.5 \times 10^4$ (and $\mathrm{Re}_\theta = 251$), but is attenuated as the Reynolds numbers increase, which supports the latter hypothesis, and indicates the presence, hence the

mutual interactions, of large-scale structures of strength decreasing with the Reynolds number in the shear layers downstream of the nozzle. These results thus also raise the question of the possible disappearance of such structures in high-Reynolds-number jets typically at $\mathrm{Re}_\theta \geq 5000$ and $\mathrm{Re}_D \geq 5 \times 10^5$.

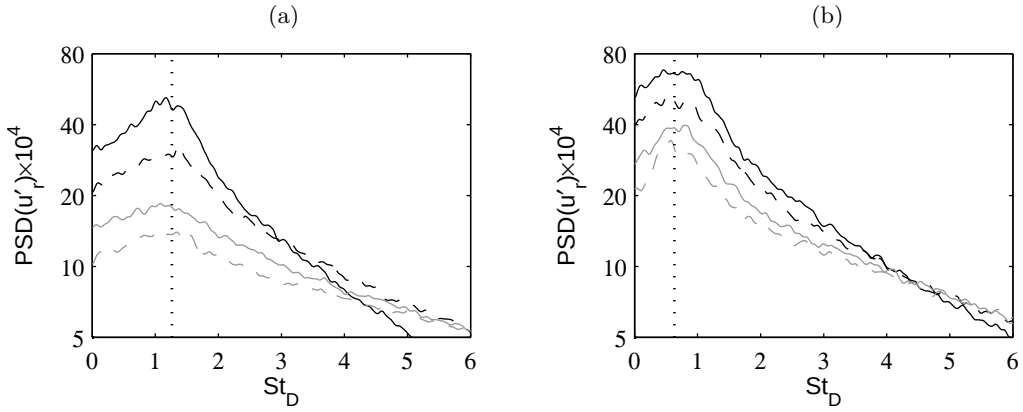

Figure 7. Power spectral densities (PSD) normalized by u_j of radial velocity u'_r, (a) at $r = r_0$ and $z = 1.5r_0$ and (b) at $r = r_0$ and $z = 4r_0$, as functions of $\mathrm{St}_D = fD/u_j$: ——— JetRe25e3, − − − JetRe50e3, ——— JetRe100e3, – – – JetRe200e3. The dotted lines indicate (a) $\mathrm{St}_\theta = f\delta_\theta(0)/u_j = 0.012$ and (b) $\mathrm{St}_\theta = 0.006$.

C. Jet flow development

Vorticity fields obtained up to $z = 25r_0$ in the four jets are represented in figure 8. They do not appear fundamentally different, especially downstream of $z \simeq 10r_0$. In the jets at higher Reynolds numbers, the mixing layers seem however to begin to interact with each other slightly farther downstream, in agreement with the reduction in shear-layer growth rate described in the previous section, which may result in longer potential cores.

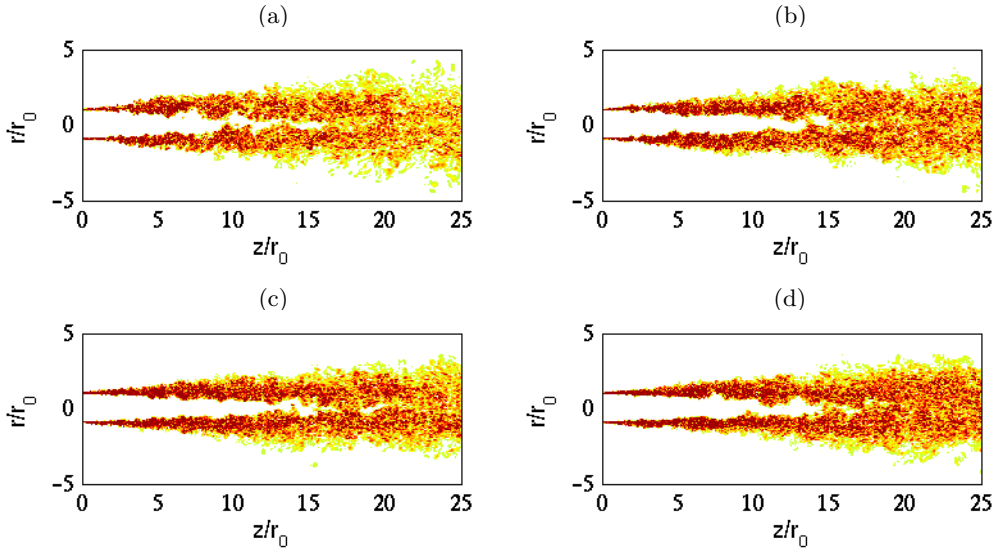

Figure 8. Snapshots in the (z, r) plane of vorticity norm $|\omega|$ in the jets up to $z = 25r_0$: (a) JetRe25e3, (b) JetRe50e3, (c) JetRe100e3, (d) JetRe200e3. The colour scale ranges up to the level of $5u_j/r_0$.

The variations of the centerline mean axial velocity u_c and of the jet half-width $\delta_{0.5}$ are presented in figures 9(a) and 9(b). With increasing Reynolds number, the velocity decay and the jet spreading both start at larger distances from the nozzle exit, leading to potential cores ending at $z_c = 13.8r_0$ in JetRe25e3, $z_c = 14.7r_0$ in JetRe50e3, and $z_c \simeq 15.8r_0$ in JetRe100e3 and JetRe200e3, where $u_c(z_c) = 0.95u_j$, as reported in table 5. Downstream of the potential core, they then appear to occur at similar rates, regardless of Re_D. For the present jets, the influence of the Reynolds number on the mean flow development is therefore relatively limited, and mainly consists of a shift in the axial direction. This behaviour is consistent with

results of previous studies in which the Reynolds number dependence of the centerline velocity decay was found to be significant[8,9,11–13,43,44] for jets at Reynolds numbers lower than 10^4, but rather weak otherwise. Poor sensitivity was observed for instance in the experiments of Deo *et al.*[13] for plane jets at width-based $\mathrm{Re}_h = 10^4$ and 1.65×10^4 (and $\mathrm{Re}_\theta = 400$ and 643), and in those of Fellouah *et al.*[14] for round jets at $\mathrm{Re}_D = 10^4$ and 3×10^4. Finally, in order to show comparisons with experimental data of the literature, measurements obtained by Lau *et al.*,[65] Arakeri *et al.*,[66] and Fleury *et al.*[67] for Mach number 0.9 round jets at Reynolds numbers $\mathrm{Re}_D \geq 5 \times 10^5$ are also depicted in figure 9. Even if the nozzle-exit conditions in the jets certainly vary, it is interesting to note that these data correspond well to the simulation results.

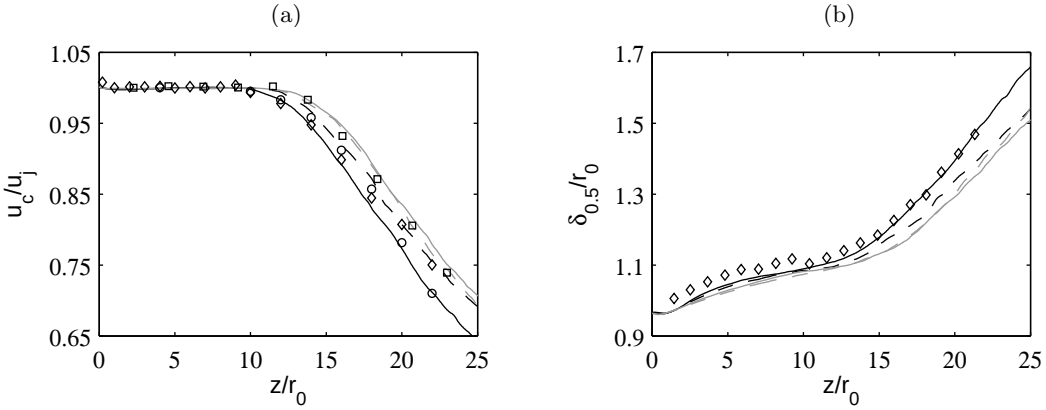

Figure 9. Variations (a) of centerline mean axial velocity u_c and (b) of jet half-width $\delta_{0.5}$: ——— JetRe25e3, − − − JetRe50e3, ——— JetRe100e3, – – – JetRe200e3. Measurements for Mach 0.9 jets at $\mathrm{Re}_D \geq 5 \times 10^5$: ○ Lau *et al.*,[65] □ Arakeri *et al.*,[66] ◇ Fleury *et al.*[67]

Table 5. Axial position of the end of the potential core z_c, and peak rms values of fluctuating velocities u'_z and u'_r on the jet axis.

	z_c/r_0	$<u'^2_z>^{1/2}/u_j$	$<u'^2_r>^{1/2}/u_j$
JetRe25e3	13.8	12.7%	9.8%
JetRe50e3	14.7	11.4%	9.4%
JetRe100e3	15.9	11.4%	9.4%
JetRe200e3	15.8	12.2%	9.4%

The variations of the centerline rms values of axial and radial fluctuating velocities are displayed in figures 10(a) and 10(b). With increasing Reynolds number, the maximum rms values are reached farther downstream, in agreement with the delay in mean flow field development, but they are not seen to change much. As shown in table 5, they are indeed close to 12% of the jet velocity for u'_z and to 9.5% for u'_r in all cases. They are nevertheless slightly higher in the jet at $\mathrm{Re}_D = 2.5 \times 10^4$, in accordance with a tendency appearing in experiments[13] and simulations[44] for low Reynolds numbers. The present turbulence intensity profiles can moreover be noticed to compare roughly with measurements available for Mach number 0.9 jets at $\mathrm{Re}_D \geq 5 \times 10^5$.

D. Acoustic fields

In order to provide a glimpse of the jet acoustic features, snapshots of the near-field fluctuating pressure obtained directly by LES are presented in figure 11. Significant differences can be observed in the sound fields. As the Reynolds number increases, the noise levels first appear to decrease. At a distance of $5r_0$ from the centerline, the peak values of pressure fluctuations between $z = 0$ and $z = 10r_0$ are for instance around 140 Pa in figure 11(a) for the jet at $\mathrm{Re}_D = 2.5 \times 10^4$, whereas they are only around 60 Pa in figure 11(d) for the jet at $\mathrm{Re}_D = 2 \times 10^5$. The structure of the sound fields is also seen to change appreciably. They clearly display low-frequency acoustic waves emitted approximately between $z = 2.5r_0$ and $z = 5r_0$ during the early stages of shear-layer development for $\mathrm{Re}_D = 2.5 \times 10^4$ and 5×10^4, whereas they show a more complicated pattern for higher Reynolds numbers.

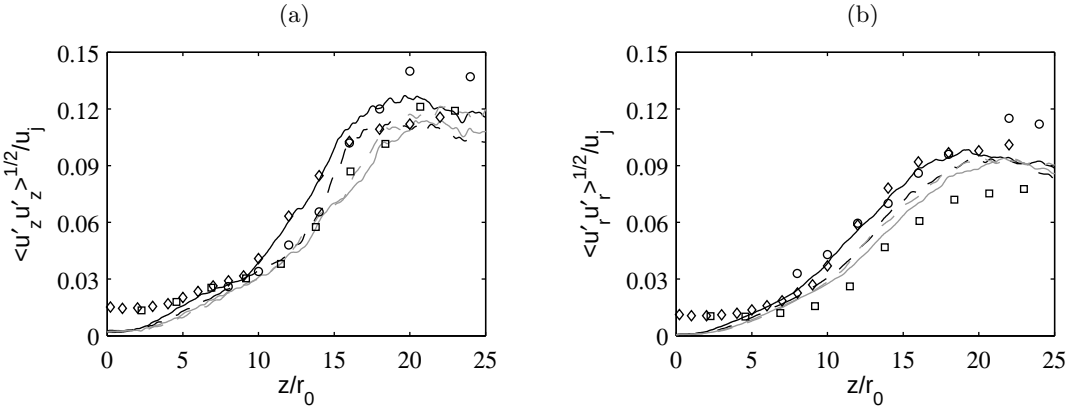

Figure 10. Variations of centerline rms values of fluctuating velocities (a) u'_z and (b) u'_r: ——— JetRe25e3, – – – JetRe50e3, ——— JetRe100e3, – – – JetRe200e3. Measurements for Mach 0.9 jets at $Re_D \geq 5 \times 10^5$: □ Arakeri *et al.*,[66] ○ Lau *et al.*,[65] ◇ Fleury *et al.*[67]

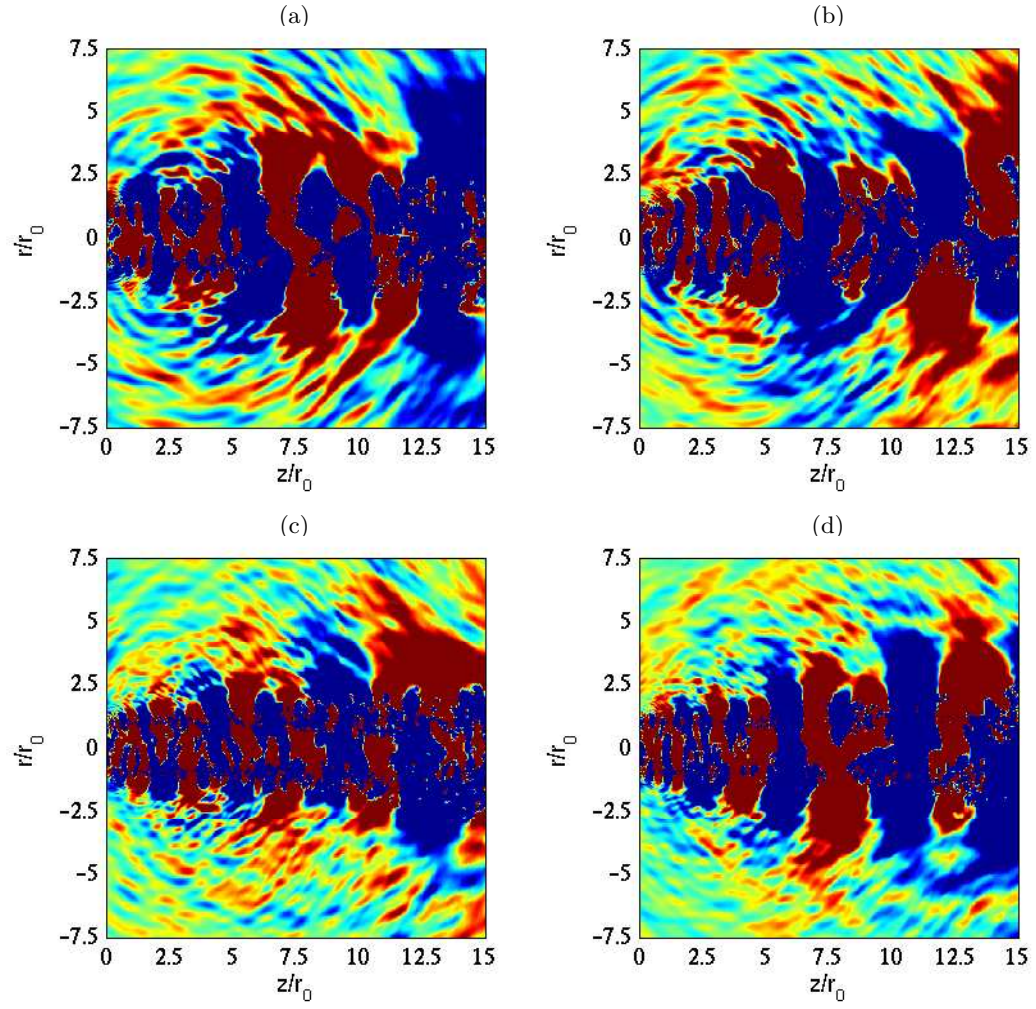

Figure 11. Snapshots in the (z, r) plane of fluctuating pressure $p - p_{amb}$ obtained by LES: (a) JetRe25e3, (b) JetRe50e3, (c) JetRe100e3, (d) JetRe200e3. The colour scale ranges from −75 to 75 Pa.

The jet far-field characteristics are examined from the pressure signals obtained at 60 radii from the nozzle exit using the wave extrapolation method documented in section II.D. The sound pressure levels determined at this distance are represented in figure 12 for angles ϕ between 30° and 110° relative to the flow direction. Compared to measurements provided by Mollo-Christensen *et al.*,[31] Lush,[68] and Bogey *et al.*[70] for Mach number 0.9 jets at $\mathrm{Re}_D \geq 5 \times 10^5$, they are found to be higher for all radiation angles. They however decrease with the Reynolds number, reducing the discrepancy with respect to the experimental data for JetRe100e3 and JetRe200e3. In the sideline direction at $\phi = 90°$, in particular, the simulations give values of 110.2 dB at $\mathrm{Re}_D = 2.5 \times 10^4$, 109.2 dB at $\mathrm{Re}_D = 5 \times 10^4$, and 108 dB at $\mathrm{Re}_D = 10^5$ and 2×10^5, whereas the measurements at $\mathrm{Re}_D \geq 5 \times 10^5$ range from 105.8 to 106.8 dB.

These variations of the sound levels with the Reynolds number are in agreement with results available in the literature. Indeed, if an increase of the Reynolds number was shown to lead to stronger noise for initially laminar free shear flows at low Reynolds numbers, namely jets[30,41,45] at $\mathrm{Re}_D \leq 10^4$ and mixing layers[46] at $\mathrm{Re}_\theta \leq 500$, noise reduction arose in a few experiments on circular jets at moderate Reynolds numbers as in this study. This trend was for instance clearly identified by Viswanathan[35] for hot jets at $\mathrm{Re}_D \leq 4 \times 10^5$. It seems also, and especially, to apply to the tripped jets of Zaman[15] at $\mathrm{Re}_D \leq 2 \times 10^5$, for which the nozzle-exit parameters $\delta_\theta(0)/r_0 \simeq 0.018$ and $u'_e/u_j \simeq 0.09$ were nearly constant and similar to those specified in the present jets. This is suggested by the fact that, with decreasing Reynolds number, the sound levels of Zaman's jets rose above the levels extrapolated from high-Reynolds-number data using classical power laws. Lowering the Reynolds number of initially highly disturbed jets at moderate Re_D thus appears to increase the sound levels with respect to the asymptotically lower levels observed for high Reynolds numbers. The jets most probably generate additional noise components, resulting from the evolutions of the large-scale turbulent structures developing in the shear layers when the effects of molecular viscosity intensify, as described in section III.B.

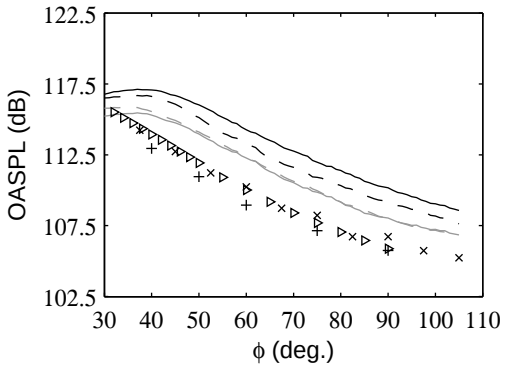

Figure 12. Overall sound pressure levels (OASPL) at $60r_0$ from the pipe exit, as a function of the angle ϕ relative to the jet direction: ——— JetRe25e3, − − − JetRe50e3, ——— JetRe100e3, – – – JetRe200e3. Measurements for jets at $\mathrm{Re}_D \geq 5 \times 10^5$: + Mollo-Christensen *et al.*,[31] × Lush,[68] ▷ Bogey *et al.*[70]

The pressure spectra obtained at $60r_0$ from the nozzle exit at the angles $\phi = 30°$, 40°, 60° and 90° relative to the jet direction are finally represented in figure 13, together with measurements of Tanna[69] and Bogey *et al.*[70] for Mach number 0.9 jets at $\mathrm{Re}_D \geq 7.8 \times 10^5$. The Strouhal number $\mathrm{St}_D = 0.7$, corresponding to $\mathrm{St}_\theta = 0.006$, which is half the frequency initially predominant in the shear layers as shown in figure 7, is also drawn. With increasing Reynolds number, as noticed previously for the far-field directivity, the noise levels decrease by about 2 dB over the Re_D range considered, yielding spectra progressively closer to the experimental spectra at the four radiation angles.

At $\phi = 30°$ and 40°, in figures 13(a) and 13(b), noise reduction is significant for $\mathrm{St}_D \geq 0.5$, but rather limited for lower Strouhal numbers. The jet noise components around $\mathrm{St}_D = 0.15$ dominating in the downstream direction therefore turn out to be weakly sensitive to Reynolds number, as found in previous numerical studies.[45] At $\phi = 90°$, in figure 13(d), the sound levels are on the contrary reduced for all frequencies. The extra hump observed for $\mathrm{St}_D \leq 0.5$ for JetRe25e3 and JetRe50e3, as is the case in the sideline spectra obtained by Viswanathan[35] for hot jets at similar Reynolds numbers, is in particular attenuated, leading to a good agreement with the measurements for JetRe100e3 and JetRe200e3 for lower frequencies. The noise components for $\mathrm{St}_D \geq 0.5$ are also damped, but there remains a slight overestimation by 2-3 dB with respect to the experimental data for the higher Reynolds number jets, as for the tripped jets of Zaman[15]

with comparable nozzle-exit conditions. As discussed in recent papers,[37,48] this can be attributed to the persistence of weak coherent-like vortical structures in the present jets, whose Reynolds numbers $\mathrm{Re}_D \simeq 10^5$ are about one order of magnitude lower than the values usually encountered in experiments. Note finally that the additional noise components radiated by the jets are roughly centered, especially at $\phi = 90^o$, around the Strouhal number value of $\mathrm{St}_D = 0.7$ which would indicate a first stage of vortex pairings downstream of the nozzle. This further supports the assertion that they are generated by the interactions of large-scale turbulent structures in the shear layers.

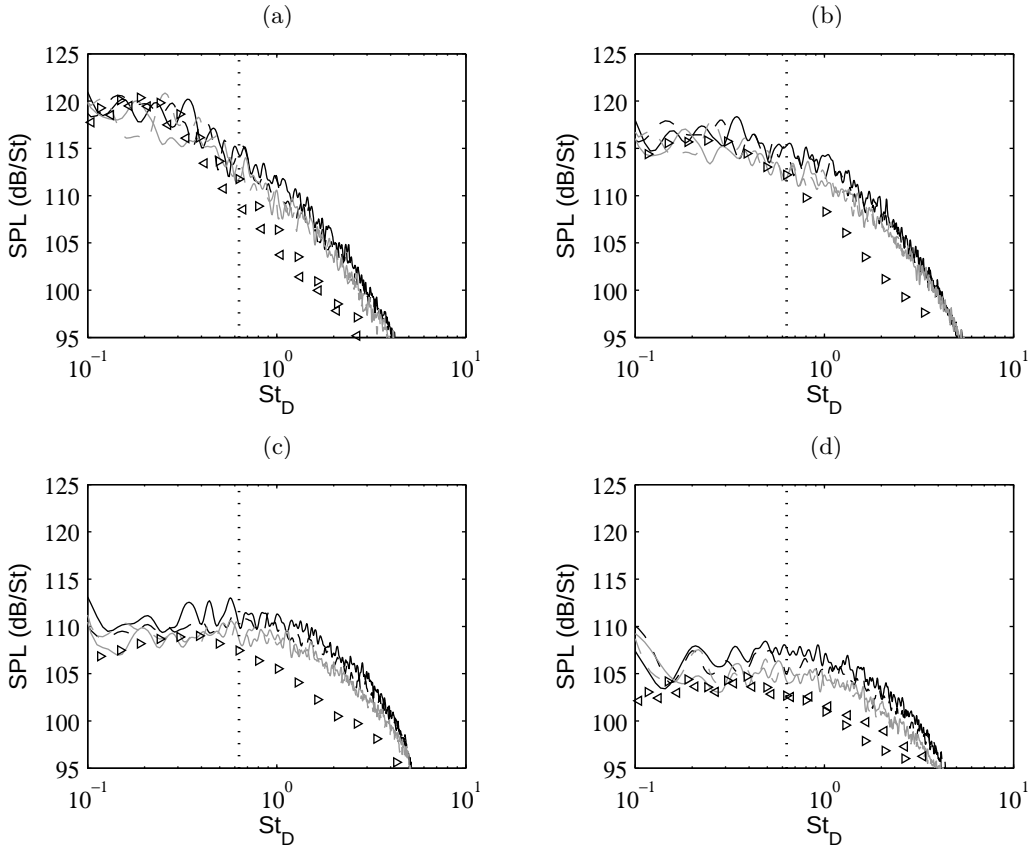

Figure 13. Sound pressure levels (SPL) at $60r_0$ from the jet exit, as a function of $\mathrm{St}_D = fD/u_j$, at the angles of (a) $\phi = 30^o$, (b) 40^o, (c) 60^o and (d) 90^o: ——— JetRe25e3, − − − JetRe50e3, ——— JetRe100e3, − − − JetRe200e3. The dotted lines indicate the frequency $\mathrm{St}_\theta = f\delta_\theta(0)/u_j = 0.006$. Measurements for jets at $\mathrm{Re}_D \geq 7.8 \times 10^5$: ◁ Tanna,[69] ▷ Bogey *et al.*[70]

IV. Conclusion

In this paper, the effects of the Reynolds number on initially highly disturbed round jets at Mach number 0.9 and moderate Reynolds numbers have been investigated. For nearly identical nozzle-exit boundary-layer parameters $H \simeq 2.3$, $\delta_\theta(0)/r_0 \simeq 0.018$ and $u'_e/u_j \simeq 0.09$, they have been found to be significant on both flow and sound fields for the ranges of diameter and momentum-thickness Reynolds numbers $2.5 \times 10^4 \leq \mathrm{Re}_D \leq 2 \times 10^5$ and $251 \leq \mathrm{Re}_\theta \leq 1830$ considered. To summarize the most important changes, jets at higher Reynolds numbers show mixing layers developing more slowly with lower turbulence intensities, have a slightly longer potential core, and produce less noise. These results are very probably due to the weakening of the shear-layer large-scale structures, and consequently of their interactions, observed as Re_D and Re_θ increase. They naturally raise the question of the threshold values of Re_D and Re_θ above which Reynolds number independence is reached. This could be studied in the future by computing jets typically at $\mathrm{Re}_D \geq 5 \times 10^5$, using many more grid points than in this work to properly deal with such high Reynolds number values.

It can be interesting to remark here that the effects of higher Reynolds numbers on jet flow and acoustic features are similar to those obtained with increasing the levels of nozzle-exit velocity disturbances.[37]

Therefore they can mutually amplify or, on the contrary, they can oppose one another when the Reynolds numbers and the exit turbulence intensities vary following opposite trends. The latter condition seems to occur for instance in a recent experiment by Zaman[17] for two jets exhausting from nozzles of same diameter but different geometries: using the so-called conic nozzle, the ratio $\delta_\theta(0)/r_0$, hence Re_θ, increased, whereas u'_e/u_j decreased at the nozzle exit. In this case, it may be difficult to know *a priori* the way in which the jet properties will vary. Finally, as mentioned above for Zaman's experiment, in jets at identical diameter and associated Reynolds number Re_D, the Reynolds numbers Re_θ are likely to differ due to discrepancies in the exit boundary-layer thickness. As a result, the latter parameter is an important jet parameter for several reasons. Its influence on initially highly disturbed jets at moderate Reynolds numbers will be examined in a further study.[71]

Acknowledgments

This work was granted access to the HPC resources of the Institut du Développement et des Ressources en Informatique Scientifique (IDRIS) under the allocation 2011-020204 made by GENCI (Grand Equipement National de Calcul Intensif).

References

[1]Sato, H., "The stability and transition of a two-dimensional jet," *J. Fluid Mech.*, Vol. 7, No. 1, 1964, pp. 53-80.

[2]Mollö-Christensen, E. and Narasimha, R., "Sound emission from jets at high subsonic velocities," *J. Fluid Mech.*, Vol. 8, No. 1, 1960, pp. 49-60.

[3]Crighton, D.G., "Acoustics as a branch of fluid mechanics," *J. Fluid Mech.*, Vol. 106, 1981, pp. 261-298.

[4]Hussain, A.K.M.F., "Coherent structures–reality and myth," *Phys. Fluids*, Vol. 26, No. 10, 1983, pp. 2816-2850.

[5]Morris, P.J., "The spatial viscous instability of axisymmetric jets," *J. Fluid Mech.*, Vol. 77, No. 3, 1976, pp. 511529.

[6]Morris, P.J., "Viscous stability of compressible axisymmetric jets," *AIAA J.*, Vol. 21, No. 4, 1983, pp. 481482.

[7]Michalke, A., "Survey on jet instability theory," *Prog. Aerospace Sci.*, Vol. 21, 1984, pp. 159-199.

[8]Lemieux, G.P. and Oosthuizen, P.H., "Experimental study of the behaviour of plane turbulent jets at low Reynolds numbers," *AIAA J.*, Vol. 23, No. 12, 1985, pp. 1845-1846. See also AIAA Paper 84-1661.

[9]Namer, I. and Ötügen, M.V., "Velocity measurements in a plane turbulent air jet at moderate Reynolds numbers," *Exp. Fluids*, Vol. 6, 1988, pp. 387-399.

[10]Weisgraber, T.H. and Liepmann, D., "Turbulent structure during transition to self-similarity in a round jet," *Exp. Fluids*, Vol. 14, 1998, pp. 210-224.

[11]Papadopoulos, G. and Pitts, W.M., "Scaling the near-field centerline mixing behavior of axisymmetric turbulent jets," *AIAA J.*, Vol. 36, No. 9, 1998, pp. 1635-1642.

[12]Kwon, S.J. and Seo, I.W., "Reynolds number effects on the behavior of a non-buoyant round jet," *Exp Fluids*, Vol. 38, No. 6, 2005, pp. 801-812.

[13]Deo, R.C., Mi, J., and Nathan, G.J., "The influence of Reynolds number on a plane jet," *Phys. Fluids*, Vol. 20, No. 1, 2008, 075108.

[14]Fellouah, H., Ball, C.G., and Pollard, A., "Reynolds number effects within the development region of a turbulent round jet," *Int. J. Heat Mass Transfer*, Vol. 52, 2009, pp. 3943-3954.

[15]Zaman, K.B.M.Q., "Effect of initial condition on subsonic jet noise," *AIAA J.*, Vol. 23, 1985, pp. 1370-1373.

[16]Zaman, K.B.M.Q., "Far-field noise of a subsonic jet under controlled excitation," *J. Fluid Mech.*, Vol. 152, 1985, pp. 83-111.

[17]Zaman, K.B.M.Q., "Effect of nozzle exit conditions on subsonic jet noise," *17th AIAA/CEAS Aeroacoustics Conference*, 6-8 June 2011, Portland, Oregon, USA, AIAA 2011-2705.

[18]Hussain, A.K.M.F and Zedan, M.F., "Effects of the initial condition on the axisymmetric free shear layer: Effects of the initial momentum thickness," *Phys. Fluids*, Vol. 21, No. 7, 1978, pp. 1100-1112.

[19]Hussain, A.K.M.F. and Zedan, M.F., "Effects of the initial condition on the axisymmetric free shear layer: Effects of the initial fluctuation level," *Phys. Fluids*, Vol. 21, No. 9, 1978, pp. 1475-1481.

[20]Gutmark, E. and Ho, C.-M., "Preferred modes and the spreading rates of jets," *Phys. Fluids*, Vol. 26, No. 10, 1983, pp. 2932-2938.

[21]Crow, S.C. and Champagne, F.H., "Orderly structure in jet turbulence," *J. Fluid Mech.*, Vol. 48, 1971, pp. 547-591.

[22]Brown, G.L. and Roshko, A., "Density effect and large structure in turbulent mixing layers," *J. Fluid Mech.*, Vol. 64, 1974, pp. 775816.

[23]Chandrsuda, C., Mehta, R.D., Weir, A.D., and Bradshaw, P., "Effect of free stream turbulence on large structure in turbulent mixing layer," *J. Fluid Mech.*, Vol. 85, No. 4, 1978, pp. 693-704.

[24]Wygnanski, I., Oster, D., Fiedler, H., and Dziomba, B., "On the perseverance of a quasi-two-dimensional eddy-structure in a turbulent mixing layer," *J. Fluid Mech.*, Vol. 93, No. 2, 1979, pp. 325-335.

[25]Zaman, K.B.M.Q. and Hussain, A.K.M.F., "Vortex pairing in a circular jet under controlled excitation. Part 1. General jet response," *J. Fluid Mech.*, Vol. 101, No. 3, 1980, pp. 449-491.

[26]Zaman, K.B.M.Q. and Hussain, A.K.M.F., "Natural large-scale structures in the axisymmetric mixing layer," *J. Fluid Mech.*, Vol. 138, 1984, pp. 325-351.

[27]Tam, C.K.W., "Supersonic jet noise," *Annu. Rev. Fluid Mech.*, Vol. 27, 1995, pp. 17-43.

[28]Morrison, G.L. and McLaughlin, D.K., "Noise generation by instabilities in low Reynolds number supersonic jets," *J. Sound. Vib.*, Vol. 65, No. 2, 1979, pp. 177-191.

[29]Troutt, T.R. and McLaughlin, D.K., "Experiments on the flow and acoustic properties of a moderate-Reynolds-number supersonic jet," *J. Fluid Mech.*, Vol. 116, 1982, pp. 123-156.

[30]Stromberg, J.L., McLaughlin, D.K., and Troutt, T.R., "Flow field and acoustic properties of a Mach number 0.9 jet at a low Reynolds number," *J. Sound. Vib.*, Vol. 72, No. 2, 1980, pp. 159-176.

[31]Mollo-Christensen, E., Kolpin, M.A., and Martucelli, J.R., "Experiments on jet flows and jet noise far-field spectra and directivity patterns," *J. Fluid Mech.*, Vol. 18, No. 2, 1964, pp. 285-301.

[32]Yamamoto, K. and Arndt, R.E.A., "Peak Strouhal frequency of subsonic jet noise as a function of Reynolds number," *AIAA 12th Fluid and Plasma Dynamics Conference*, Williamsburg, VA, July 1979, AIAA Paper 79-1525.

[33]Long, D.F. and Arndt, R.E.A., "Jet noise at low Reynolds number," *AIAA J.*, Vol. 22, No. 2, 1984, pp. 187-193.

[34]Bridges, J.E. and Hussain, A.K.M.F., "Roles of initial conditions and vortex pairing in jet noise," *J. Sound Vib.*, Vol. 117, No. 2, 1987, pp. 289-311.

[35]Viswanathan, K., "Aeroacoustics of hot jets," *J. Fluid Mech.*, Vol. 516, 2004, pp. 39-82.

[36]Bogey, C. and Bailly, C., "Influence of nozzle-exit boundary-layer conditions on the flow and acoustic fields of initially laminar jets," *J. Fluid Mech.*, Vol. 663, 2010, pp. 507-539

[37]Bogey, C., Marsden, O., and Bailly, C., "Influence of initial turbulence level on the flow and sound fields of a subsonic jet at a diameter-based Reynolds number of 10^5," submitted to *J. Fluid Mech.*, 2011. See also AIAA 2011-2837.

[38]Colonius, T. and Lele, S.K., "Computational aeroacoustics: progress on nonlinear problems of sound generation," *Progress in Aerospace Sciences*, Vol. 40, 2004, pp. 345-416.

[39]Bailly, C. and Bogey, C., "Contributions of CAA to jet noise research and prediction," *Int. J. Comput. Fluid Dyn.*, Vol. 18, No. 6, 2004, pp. 481-491.

[40]Wang, M., Freund J.B., and Lele, S.K., "Computational prediction of flow-generated sound," *Annu. Rev. Fluid. Mech.*, Vol. 38, 2006, pp. 483-512.

[41]Freund, J.B., "Noise sources in a low-Reynolds-number turbulent jet at Mach 0.9," *J. Fluid Mech.*, Vol. 438, 2001, pp. 277-305.

[42]Bogey, C., Bailly, C., and Juvé, D., "Noise investigation of a high subsonic, moderate Reynolds number jet using a compressible LES," *Theoret. Comput. Fluid Dynamics*, Vol. 16, No. 4, 2003, pp. 273-297.

[43]Klein, M., Sadiki, A., and Janicka, J., "Investigation of the influence of the Reynolds number on a plane jet using direct numerical simulation," *Int. J. Heat Fluid Flow*, Vol. 24, 2003, pp. 785-794.

[44]Bogey, C. and Bailly, C., "Large Eddy Simulations of transitional round jets: influence of the Reynolds number on flow development and energy dissipation," *Phys. Fluids*, Vol. 18, No. 6, 2006, 065101.

[45]Bogey, C. and Bailly, C., "Investigation of downstream and sideline subsonic jet noise using Large Eddy Simulations," *Theoret. Comput. Fluid Dynamics*, Vol. 20, No. 1, 2006, pp. 23-40.

[46]Kleinman, R.R. and Freund, J.B., "The sound from mixing layers simulated with different ranges of turbulent scales," *Phys. Fluids*, Vol. 20, No. 10, 2008, 101503.

[47]Kim, J. and Choi, H., "Large eddy simulation of a circular jet: effect of inflow conditions on the near field," *J. Fluid Mech.*, Vol. 620, 2009, pp. 383-411.

[48]Bogey, C., Marsden, O., and Bailly, C., "Large-Eddy Simulation of the flow and acoustic fields of a Reynolds number 10^5 subsonic jet with tripped exit boundary layers," *Phys. Fluids*, Vol. 23, No. 3, 2011, 035104.

[49]Bogey, C., Marsden, O., and Bailly, C., "On the spectra of nozzle-exit velocity disturbances in initially nominally turbulent jets," *Phys. Fluids*, Vol. 23, No. 9, 2011, 091702.

[50]Mohseni, K. and Colonius, T., "Numerical treatment of polar coordinate singularities," *J. Comput. Phys.*, Vol. 157, No. 2, 2000, pp. 787-795.

[51]Bogey, C., de Cacqueray, N., and Bailly, C., "Finite differences for coarse azimuthal discretization and for reduction of effective resolution near origin of cylindrical flow equations," *J. Comput. Phys.*, Vol. 230, No. 4, 2011, pp. 1134-1146.

[52]Bogey, C. and Bailly, C., "A family of low dispersive and low dissipative explicit schemes for flow and noise computations," *J. Comput. Phys.*, Vol. 194, No. 1, 2004, pp. 194-214.

[53]Bogey, C., de Cacqueray, N., and Bailly, C., "A shock-capturing methodology based on adaptative spatial filtering for high-order non-linear computations," *J. Comput. Phys.*, Vol. 228, No. 5, 2009, pp. 1447-1465.

[54]Berland, J., Bogey, C., Marsden, O., and Bailly, C., "High-order, low dispersive and low dissipative explicit schemes for multi-scale and boundary problems," *J. Comput. Phys.*, Vol. 224, No. 2, 2007, pp. 637-662.

[55]Tam, C.K.W and Dong, Z., "Radiation and outflow boundary conditions for direct computation of acoustic and flow disturbances in a nonuniform mean flow., *J. Comput. Acoust.*, Vol. 4, No. 2,, 1996, pp. 175201.

[56]Bogey, C. and Bailly, C., "Three-dimensional non reflective boundary conditions for acoustic simulations: far-field formulation and validation test cases," *Acta Acustica*, Vol. 88, No. 4, 2002, pp. 463-471.

[57]Bogey, C. and Bailly, C., "Large eddy simulations of round jets using explicit filtering with/without dynamic Smagorinsky model," *Int. J. Heat and Fluid Flow*, Vol. 27, No. 4, 2006, pp. 603-610.

[58]Bogey, C. and Bailly, C., "Turbulence and energy budget in a self-preserving round jet: direct evaluation using large-eddy simulation," *J. Fluid Mech.*, Vol. 627, 2009.

[59]Bogey, C., Barré, S., Juvé, D., and Bailly, C., "Simulation of a hot coaxial jet : direct noise prediction and flow-acoustics correlations," *Phys. Fluids*, Vol. 21, No. 3, 2009, 035105.

[60]Ahuja, K.K., Tester, B.J., and Tanna, H.K., "Calculation of far field jet noise spectra from near field measurements with true source location," *J. Sound Vib.*, Vol. 116, No. 3, 1987, pp. 415-426.

[61]Eggels, J.G.M., Unger, F., Weiss, M.H., Westerweel, J., Adrian, R.J., Friedrich, R., and Nieustadt, F.T.M., "Fully developed turbulent pipe flow: a comparison between direct numerical simulation and experiment," *J. Fluid Mech.*, Vol. 268, 1994, pp. 175-209.

[62]Tomkins, C.D. and Adrian, R.J., "Energetic spanwise modes in the logarithmic layer of a turbulent boundary layer," *J. Fluid Mech.*, Vol. 545, 2005, pp. 141-162.

[63]Tomkins, C.D. and Adrian, R.J., "Spanwise structure and scale growth in turbulent boundary layers," *J. Fluid Mech.*, Vol. 490, 2003, pp. 37-74.

[64]Husain, Z.D. and Hussain, A.K.M.F., "Axisymmetric mixing layer: influence of the initial and boundary conditions," *AIAA J.*, Vol. 17, No. 1, 1979, pp. 48-55.

[65]Lau, J.C., Morris, P.J., and Fisher, M.J., "Measurements in subsonic and supersonic free jets using a laser velocimeter," *J. Fluid Mech.*, Vol. 93, No. 1, 1979, pp. 1-27.

[66]Arakeri, V.H., Krothapalli, A., Siddavaram, V., Alkislar, M.B., and Lourenco, L., "On the use of microjets to suppress turbulence in a Mach 0.9 axisymmetric jet," *J. Fluid Mech.*, Vol. 490, 2003, pp. 75-98.

[67]Fleury, V., Bailly, C., Jondeau, E., Michard, M., and Juvé, D., "Space-time correlations in two subsonic jets using dual-PIV measurements," *AIAA J.*, Vol. 46, No. 10, 2008, pp. 2498-2509.

[68]Lush, P.A., "Measurements of subsonic jet noise and comparison with theory," *J. Fluid Mech.*, Vol. 46, No. 3, 1971, pp. 477-500.

[69]Tanna, H.K., "An experimental study of jet noise. Part I: Turbulent mixing noise," *J. Sound Vib.*, Vol. 50, No. 3, 1977, pp. 405-428.

[70]Bogey, C., Barré, S., Fleury, V., Bailly, C., and Juvé, D., "Experimental study of the spectral properties of near-field and far-field jet noise," *Int. J. of Aeroacoustics*, Vol. 6, No. 2, 2007, pp. 73-92.

[71]Bogey, C., Marsden, O., and Bailly, C., "Effects of initial shear-layer thickness on turbulent subsonic jets at moderate Reynolds numbers," *18th AIAA/CEAS Aeroacoustics Conference*, 4-6 June 2012, Colorado Springs, CO, USA.